PROCEEDINGS OF SCIENCE

BSM fits for $b \to s\ell\ell$ decays

B. Capdevila
Universitat Autònoma de Barcelona,
08193 Bellaterra, Spain

S. Descotes-Genon*
Laboratoire de Physique Théorique (UMR 8627), CNRS, Univ. Paris-Sud,
Université Paris-Saclay, 91405 Orsay Cedex, France

L. Hofer
Universitat de Barcelona (UB), Martí Franquès 1,
08028 Barcelona, Spain

J. Matias
Universitat Autònoma de Barcelona,
08193 Bellaterra, Spain

J. Virto
Albert Einstein Center for Fundamental Physics, Institute for Theoretical Physics,
University of Bern, CH-3012 Bern, Switzerland.

Recently, the LHC has found several anomalies in exclusive semileptonic $b \to s\ell^+\ell^-$ decays, which can be analysed through a global analysis of the relevant decay modes. After a discussion of the hadronic uncertainties entering the theoretical predictions, we present the interpretation of the data in terms of generic new physics scenarios and we discuss model-independent fits of the corresponding Wilson coefficients to the data. In some cases, the best fit point is preferred over the Standard Model by a global significance of 4σ or more. Based on these results, the discrimination between high-scale new physics and low-energy QCD effects as well as the study of lepton-flavour universality violation are discussed.

16th International Conference on B-Physics at Frontier Machines
2-6 May 2016
Marseille, France

*Speaker.

PoS(BEAUTY2016)044

1. Introduction

The flavour-changing neutral current (FCNC) transition $b \to s\ell^+\ell^-$ can be probed through various decay channels, currently studied in detail at the LHC in the LHCb, CMS and ATLAS experiments, as well as at Belle. Recent experimental results have shown interesting deviations from the Standard Model (SM). The LHCb analysis [1] of the $3\,\text{fb}^{-1}$ data on $B \to K^*\mu^+\mu^-$ in particular confirms a $\sim 3\sigma$ anomaly in two large K^*-recoil bins of the angular observable P_5' [2] that was already present in the 2013 results with $1\,\text{fb}^{-1}$ [3] and subsequently confirmed by the Belle experiment [4]. The observable $R_K = Br(B \to K\mu^+\mu^-)/Br(B \to Ke^+e^-)$ was measured by LHCb [5] in the dilepton mass range from 1 to 6 GeV^2 as $0.745^{+0.090}_{-0.074} \pm 0.036$, corresponding to a 2.6σ tension with its SM value predicted to be equal to 1 (to a high accuracy). Finally, the LHCb results [6] on the branching ratio of $B_s \to \phi\mu^+\mu^-$ exhibit deviations in two large-recoil bins.

The appearance of several tensions in different $b \to s\ell^+\ell^-$ channels is interesting since all these observables are sensitive to the same couplings $\mathscr{C}_{7,9,10}^{(\prime)}$ induced by the local four-fermion operators in the effective Hamiltonian approach (see Fig. 1)

$$\mathscr{O}_9^{(\prime)} = \frac{\alpha}{4\pi}[\bar{s}\gamma^\mu P_{L(R)}b][\bar{\mu}\gamma_\mu\mu], \quad \mathscr{O}_{10}^{(\prime)} = \frac{\alpha}{4\pi}[\bar{s}\gamma^\mu P_{L(R)}b][\bar{\mu}\gamma_\mu\gamma_5\mu], \quad \mathscr{O}_7^{(\prime)} = \frac{\alpha}{4\pi}m_b[\bar{s}\sigma_{\mu\nu}P_{R(L)}b]F^{\mu\nu},$$
$$\mathscr{C}_9^{\text{SM}}(\mu_b) = 4.07, \qquad \mathscr{C}_{10}^{\text{SM}}(\mu_b) = -4.31, \qquad \mathscr{C}_7^{\text{SM}}(\mu_b) = -0.29, \quad (1.1)$$

where $P_{L,R} = (1 \mp \gamma_5)/2$, m_b denotes the b quark mass, $\mu_b = 4.8$ GeV, and primed operators have vanishing or negligible Wilson coefficients in the SM. It is natural to ask whether a new physics (NP) contribution to these couplings could account for all the tensions at once, coming from particular extensions (Z' bosons, leptoquarks…) inducing contributions to some Wilson coefficients.

The couplings $\mathscr{C}_{7,9,10}^{(\prime)}$ can be constrained through various observables in radiative and (semi) leptonic $B_{(s)}$ decays, each of them sensitive to a different subset of coefficients (see Fig. 1). The investigation of potential NP effects thus requires a combined study of these observables including correlations. We will first discuss the hadronic uncertainties entering the theoretical predictions of the relevant observables for exclusive decays (where the deviations appear), before describing the results of global fits performed to unravel such effects.

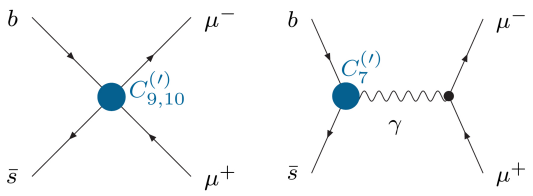

processes	$\mathscr{C}_7^{(\prime)}$	$\mathscr{C}_9^{(\prime)}$	$\mathscr{C}_{10}^{(\prime)}$
$B \to X_s\gamma$, $B \to K^*\gamma$	✓		
$B \to X_s\mu^+\mu^-$	✓	✓	✓
$B_s \to \mu^+\mu^-$			✓
$B_{(s)} \to (K^{(*)}, \phi)\mu^+\mu^-$	✓	✓	✓

Figure 1: Effective couplings $\mathscr{C}_{7,9,10}^{(\prime)}$ contributing to $b \to s\ell^+\ell^-$ transitions and sensitivity of the various radiative and (semi)leptonic $B_{(s)}$ decays to them.

2. Hadronic uncertainties

Predictions for exclusive semileptonic B decays are plagued by QCD effects of perturbative and non-perturbative nature. At leading order (LO) in the effective theory, predictions involve tree-level diagrams with insertions of the operators $\mathscr{O}_{7,9,10}$ (generated at one loop in the SM), as well as

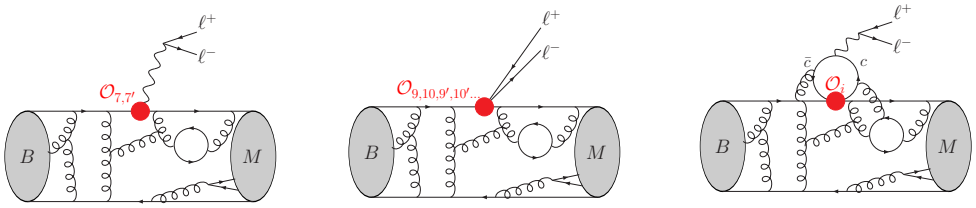

Figure 2: Illustration of factorisable (first two diagrams) and non-factorisable (third diagram) QCD corrections to exclusive $B \to M\ell^+\ell^-$ matrix elements.

one-loop diagrams with an insertion of the charged-current operator $\mathcal{O}_2 = [\bar{s}\gamma^\mu P_L c][\bar{c}\gamma_\mu P_L b]$ (generated at tree level in the SM). In the first case the leptonic and the hadronic currents factorise, and QCD corrections are constrained to the hadronic $B \to M$ current (first two diagrams in Fig. 2). This class of *factorisable QCD corrections* thus forms part of the hadronic form factors parametrising the $B \to M$ transition. Contributions of the second type receive *non-factorisable QCD corrections* (third diagram in Fig. 2) that cannot be absorbed into form factors. We will briefly discuss both effects in the following sections.

2.1 Form factor uncertainties

The form factors are available from lattice QCD as well as from light-cone sum rule (LCSR) calculations, with the former being suited for the region of high $q^2 > 15\,\text{GeV}^2$ and the latter for the region of low $q^2 < 8\,\text{GeV}^2$. Since the form factors introduce a dominant source of theoretical uncertainties, it is desirable to reduce the sensitivity to them as much as possible. For $B \to V\ell^+\ell^-$ decays, with V being a vector meson, this can be achieved in the low-q^2 region by exploiting large-recoil symmetries of QCD. At LO in α_s and Λ/m_b, these symmetries enforce certain relations among the seven hadronic form factors $V, A_1, A_2, A_0, T_1, T_2, T_3$, like

$$\frac{m_B(m_B+m_{K^*})A_1 - 2E(m_B-m_{K^*})A_2}{m_B^2 T_2 - 2E m_B T_3]} = 1 + \mathcal{O}(\alpha_s, \Lambda/m_b), \tag{2.1}$$

where E denotes the energy of the K^* meson. The coefficients of the differential angular distribution can be used to build observables that involve ratios like eq. (2.1). This line, originated in Refs. [7], was followed by many references [2, 8, 9]. The resulting optimised observables $P_i^{(\prime)}$ exhibit a mild form factor dependence, suppressed by powers of α_s and Λ/m_b.

For the cancellation of the form factor uncertainties in ratios like the one in eq. (2.1), it is essential to control the correlations among the errors of the different form factors. These correlations can be taken into account via two different approaches: either they can be assessed directly from a LCSR calculation (Ref. [10] provides LCSR form factors with correlation matrices) [full form factor approach], or they can be implemented resorting to the large-recoil symmetry relations [soft form factor approach]. Whereas the former method is limited to a particular set of form factors (currently only Ref. [10]) and hence sensitive to details of the corresponding calculation, the latter method determines the correlations in a model-independent way from first principles and can thus also be applied to different sets of form factors like the ones from Ref. [11], where no correlations were provided. As a drawback, correlations are obtained from large-recoil symmetries only up to Λ/m_b corrections which have to be estimated.

2.2 Uncertainties from $c\bar{c}$ loops

Long-distance charm-loop effects (third diagram in Fig. 2) can mimic the effect of an effective coupling $\mathscr{C}_9^{c\bar{c}}$ and have been suggested as a solution of the anomaly in $B \to K^* \mu^+ \mu^-$ [12, 13]. Due to the non-local structure of these corrections, their contribution is expected to have a non-constant q^2-dependence, where q^2 is the squared invariant masses of the lepton pair. Together with the perturbative SM contribution $\mathscr{C}_{9\,\mathrm{SM\,pert}}^{\mathrm{eff}}$ and a potential constant NP coupling $\mathscr{C}_9^{\mathrm{NP}}$, it can be cast into an effective Wilson coefficient

$$\mathscr{C}_9^{\mathrm{eff\,i}}(q^2) = \mathscr{C}_{9\,\mathrm{SM\,pert.}}^{\mathrm{eff}}(q^2) + \mathscr{C}_9^{\mathrm{NP}} + \mathscr{C}_9^{c\bar{c}\,i}(q^2), \tag{2.2}$$

with a different $\mathscr{C}_9^{c\bar{c}\,i}$ and hence also a different $\mathscr{C}_9^{\mathrm{eff\,i}}$ for the three transversity amplitudes $i = 0, \|, \perp$. The evaluation of this long-distance contribution is difficult, especially close to the region of charmonium resonances. Currently, only a partial calculation [11] exists, based on light-cone sum rules combined with a dispersion relation: the result $\mathscr{C}_{9\,\mathrm{KMPW}}^{c\bar{c}\,i}$ actually enhances the anomalies. We will come back later to other approaches to this question.

3. Global analysis of $b \to s\ell\ell$ data

3.1 Global fits

The rare $b \to s\ell\ell$ decays have been known for a long time to have a potential sensitivity to New Physics, and the interest of a global analysis of various hadronic channels and observables was realised much before the advent of LHCb data [14]. The first analysis performed in this spirit and exploiting the LHCb 2013 data [15] pointed to a large negative contribution to the Wilson coefficient $\mathscr{C}_9$. This general picture was confirmed later on by other groups, using different/additional observables, different theoretical input for the form factors, etc. (see, e.g., Refs. [16, 17]).

We first outline the results of our analysis in Ref. [18] which improves Ref. [15] in many aspects: it includes the latest experimental results of all relevant decays (using the LHCb data for the exclusive), it relies on refined techniques to estimate uncertainties originating from power corrections to the hadronic form factors and from non-perturbative charm loops, and it takes into account experimental and theoretical correlations. Our reference fit includes the branching ratios and angular observables for $B \to K^* \mu^+ \mu^-$ and $B_s \to \phi \mu^+ \mu^-$, the branching ratios of the charged and neutral modes $B \to K \mu^+ \mu^-$, the branching ratios of $B \to X_s \mu^+ \mu^-$, $B_s \to \mu^+ \mu^-$ and $B \to X_s \gamma$, as well as the isospin asymmetry A_I and the time-dependent CP asymmetry $S_{K^*\gamma}$ of $B \to K^* \gamma$. Both low- and large-recoil data (but not the resonance region) are included for the exclusive modes.

For the predictions, we use the lattice form factors from Refs. [19] in the low-recoil region, and the LCSR form factors from Ref. [11] (except for $B_s \to \phi$ where Ref. [10] is used). We use the soft form factor approach to include the theoretical correlations among form factors at large recoil. For factorisable power corrections, we follow the strategy that was developed in Ref. [20] refining a method first proposed in Ref. [21]. We assume a generic size of 10% factorisable power corrections to the form factors, which is consistent with the results that are obtained from a fit to the particular LCSR form factors from Refs. [11, 10]. For charm-loop contributions, we assume that the partial result of Ref. [11] is representative for the order of magnitude of the total contribution. When we

Coefficient	Best fit	1σ	3σ	Pull_{SM}
$\mathscr{C}_7^{\text{NP}}$	-0.02	$[-0.04,-0.00]$	$[-0.07,0.03]$	1.2
$\mathscr{C}_9^{\text{NP}}$	-1.09	$[-1.29,-0.87]$	$[-1.67,-0.39]$	4.5
$\mathscr{C}_{10}^{\text{NP}}$	0.56	$[0.32,0.81]$	$[-0.12,1.36]$	2.5
$\mathscr{C}_{7'}^{\text{NP}}$	0.02	$[-0.01,0.04]$	$[-0.06,0.09]$	0.6
$\mathscr{C}_{9'}^{\text{NP}}$	0.46	$[0.18,0.74]$	$[-0.36,1.31]$	1.7
$\mathscr{C}_{10'}^{\text{NP}}$	-0.25	$[-0.44,-0.06]$	$[-0.82,0.31]$	1.3
$\mathscr{C}_9^{\text{NP}} = -\mathscr{C}_{10}^{\text{NP}}$	-0.68	$[-0.85,-0.50]$	$[-1.22,-0.18]$	4.2
$\mathscr{C}_9^{\text{NP}} = -\mathscr{C}_{9'}^{\text{NP}}$	-1.06	$[-1.25,-0.85]$	$[-1.60,-0.40]$	4.8

Table 1: Results of one-parameter fits for the Wilson coefficients $\mathscr{C}_i$ considering only $b \to s\mu\mu$ transitions. From Ref. [18].

compute observables in the large-recoil region, we assign an error to unknown charm-loop effects varying $\mathscr{C}_9^{c\bar{c}\,i}(q^2) = s_i\, \mathscr{C}_{9\,\text{KMPW}}^{c\bar{c}\,i}(q^2)$ with $-1 \le s_i \le 1$ for each transversity $i = 0, \perp, ||$.

Starting from a model hypothesis with free parameters for some Wilson coefficients $\{\mathscr{C}_i^{\text{NP}}\}$, we perform a frequentist fit, including experimental and theoretical correlation matrices. Tab. 1 summarises the results for various one-parameter scenarios. In the last column we give the SM-pull for each scenario, i.e. by how many sigmas the best fit point is preferred over the SM point $\{\mathscr{C}_i^{\text{NP}}\} = 0$ in the given scenario. A scenario with a large SM-pull leads to a big improvement over the SM and a better description of the data. Going through the various scenarios, a large negative $\mathscr{C}_9^{\text{NP}}$ is required to explain the data. The one-dimensional scenario with only this coefficient leads to a satisfying goodness-of-fit for $\mathscr{C}_9^{\text{NP}} \sim -1.1$. Analysing the different exclusive decay channels separately, as well as the low- and large-recoil regions, shows that each subset points to the same solution, i.e. a negative $\mathscr{C}_9^{\text{NP}}$, albeit with different significances. Several two-dimensional scenarios are also of interest, in particular for $(\mathscr{C}_9, \mathscr{C}_{10})$ and $(\mathscr{C}_9, \mathscr{C}_{9'})$. A full 6-parameter fit of $\mathscr{C}_{7,9,10}^{(\prime)\text{NP}}$ results in a SM-pull of 3.6σ, with only $\mathscr{C}_9$ deviating significantly from its SM value [18].

Earlier analyses of partial subsets of $b \to s\ell\ell$ data cannot be described here for lack of space, but we can compare the results of Ref. [18] with two recent global analyses involving similar sets of up-to-date data. Both are based on a frequentist approach, but they rely on different inputs and hypotheses from Ref. [18]. Ref. [22] exploits a different set of hadronic form factors with much smaller uncertainties [10] using the full form factor approach, it relies on different estimates for the long-distance QCD corrections, it uses exclusive data not only form LHCb but also from other LHC and B-factory experiments, and it does not exploit optimised observables but rather averaged angular coefficients. Ref. [23] uses the same set of hadronic form factors [10] within either the soft or full form factor approaches, it uses different parametrisations to assess hadronic uncertainties, it considers two different test statistics (with different coverage properties), and it deals only with LHCb data (including the results of the method of moments, affected by larger uncertainties).

Their results agree well with Ref. [18], bearing in mind the differences in the experimental inputs and the theoretical uncertainties. All analyses prefer scenarios involving a contribution to

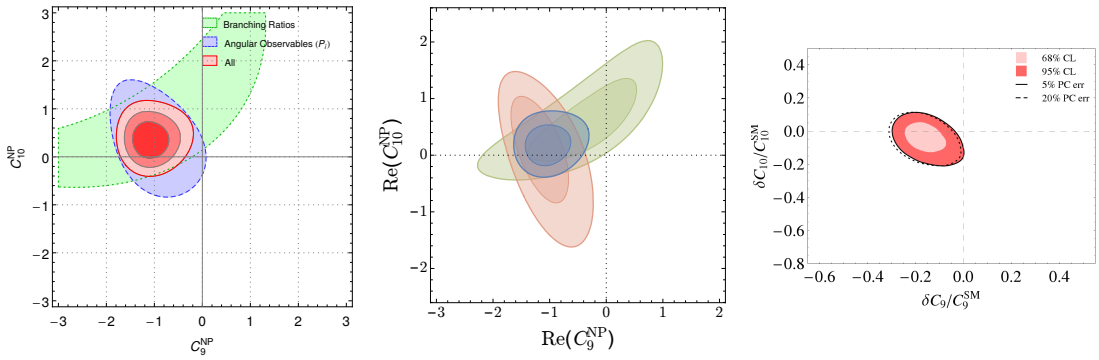

Figure 3: Results for the two-dimensional scenario with real contributions to $\mathscr{C}_9$ and $\mathscr{C}_{10}$ from Refs. [18] (left), [22] (center) and [23] (right).

$\mathscr{C}_9$ in $b \to s\mu\mu$, whereas contribution to other Wilson coefficients are only loosely bound and compatible with SM. For the one-dimensional hypothesis for a contribution $\mathscr{C}_9^{\rm NP}$ in $b \to s\mu\mu$, Ref. [22] (Ref. [23] respectively) obtains a SM-pull of 3.7 σ (4.2 σ respectively) and a 68% confidence interval of [-1.32,-0.81] ([-1.10,-0.53] respectively). The one-dimensional scenario $\mathscr{C}_9^{\rm NP} = -\mathscr{C}_{10}^{\rm NP}$ and the two-dimensional scenario $(\mathscr{C}_9^{\rm NP}, \mathscr{C}_{10}^{\rm NP})$ are favoured in all three analyses and the similarity of the outcome of the three analyses is illustrated for the latter case in Fig. 3. Both Ref. [22] and Ref. [23] also studied the role played by hadronic uncertainties (power corrections, form factor uncertainties, charm contributions): only very large contributions would be able to reproduce some of the anomalies observed in $b \to s\ell\ell$ data (without explaining $R_K \neq 1$, see below). In addition, Ref. [22] pointed out first that their fit does not favour a q^2-dependent contribution to $\mathscr{C}_9$ that would mark a significant and overlooked hadronic contribution, in agreement with the results of Ref. [18].

3.2 New physics vs. non-perturbative charm-contribution

According to Eq. (2.2), a potential NP contribution $\mathscr{C}_9^{\rm NP}$ enters amplitudes always together with a charm-loop contribution $\mathscr{C}_9^{c\bar{c}\,i}(q^2)$, spoiling an unambiguous interpretation of the fit result from the previous section in terms of NP. Whereas $\mathscr{C}_9^{\rm NP}$ does not depend on the squared invariant mass q^2 of the lepton pair, $\mathscr{C}_9^{c\bar{c}\,i}(q^2)$ is expected to exhibit a non-trivial q^2-dependence. We show in Fig. 4 on the left a bin-by-bin fit for the one-parameter scenario with a single coefficient $\mathscr{C}_9^{\rm NP}$. The results obtained in the individual bins are consistent with each other, allowing thus for $\mathscr{C}_9^{\rm NP}$ constant in the whole q^2 region, as required for an interpretation in terms of NP, though the situation is not conclusive due to the large uncertainties in the single bins.

An alternative strategy to address this question has been followed recently in Ref. [13] where fits of the q^2-dependent charm contribution $\mathscr{C}_9^{c\bar{c}\,i}(q^2)$ to the data on $B \to K^*\mu^+\mu^-$ (at low q^2) has been performed under the hypothesis of the absence of NP. A first fit imposing the results of Ref. [11] for $q^2 \leq 1$ GeV^2 yields a q^2-dependence suggestive of an unexpectedly large $c\bar{c}$ component. However, this q^2-dependence comes precisely from imposing specific, purely SM, values at low q^2 and forcing the fit to adopt a skewed and spurious q^2-dependence. A second fit, without any constraints, yields a result compatible with the results of Ref. [11] supplemented with a constant, helicity-independent, contribution, i.e., $\mathscr{C}_9^{\rm NP}$. The results in Ref. [13] do not allow to draw any

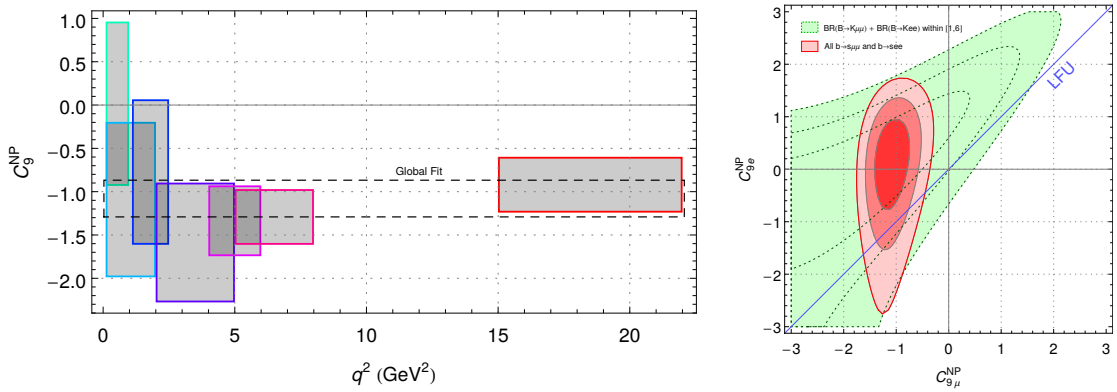

Figure 4: Left: Bin-by-bin fit of the one-parameter scenario with a single coefficient $\mathscr{C}_9^{\rm NP}$ for $b \to s\mu\mu$. Right: Fit with independent coefficients $\mathscr{C}_{9\,\mu}^{\rm NP}$ and $\mathscr{C}_{9\,e}^{\rm NP}$, for $b \to s\mu\mu$ and $b \to see$ transitions respectively. From Ref. [18].

conclusions on whether a q^2-dependent solution of the anomalies via $\mathscr{C}_9^{c\bar{c}\,i}(q^2)$ is preferred compared to a solution via a constant $\mathscr{C}_9^{\rm NP}$ since this would require a comparison of the goodness of the fit taking into account the different number of free parameters of the two parametrizations (or other equivalent tools, such as the information criterion of these two hypotheses, not considered in Ref. [13]). Moreover, we should stress that the results for the observables presented in Ref. [13] should not be interpreted as SM predictions, as they are based on a fit to the experimental data.

3.3 Lepton-flavour universality violation

Since the measurement of R_K suggests the violation of lepton-flavour universality, we also studied the situation where the muon- and the electron-components of the operators $\mathscr{C}_{9,10}^{(\prime)}$ receive independent NP contributions $\mathscr{C}_{i\,\mu}^{\rm NP}$ and $\mathscr{C}_{i\,e}^{\rm NP}$, respectively. The electron-couplings $\mathscr{C}_{i\,e}^{\rm NP}$ are constrained by adding $B \to K^{(*)}e^+e^-$ to the global fit [5, 24]. The correlated fit to $B \to K\mu^+\mu^-$ and $B \to Ke^+e^-$ simultaneously is equivalent to a direct inclusion of the observable R_K. In Fig. 4 on the right we display the result for the two-parameter fit to the coefficients $\mathscr{C}_{9\,\mu}^{\rm NP}$ and $\mathscr{C}_{9\,e}^{\rm NP}$. The fit prefers a scenario with NP coupling to $\mu^+\mu^-$ but not to e^+e^-. Under this hypothesis, the SM-pull increases by $\sim 0.5\sigma$ compared to the value in Tab. 1 for the lepton-flavour universal scenario.

We expect in a near future to have experimental analyses for electron as well as muon for the various decay modes. The comparison of these modes, and in particular ratios of branching ratios, has been shown to provide interesting and non-ambiguous information on New Physics, due to the cancellation of long-distance contributions [25]. In addition to R_K and its extensions to vector modes (R_{K^*} and R_ϕ), one can discuss how angular analyses of $B \to K^*ee$ and $B \to K^*\mu\mu$ decay modes can be combined to understand better the pattern of anomalies observed and to get a solid handle on the size of some SM long-distance contributions. In Ref. [26], we introduced the following observables: $Q_i = P_i^\mu - P_i^e$ and $B_i = J_i^\mu / J_i^e - 1$ associated with the optimised observables P_i and the angular coefficients J_i describing the geometry of the $B \to K^*\ell\ell$ decay. A measurement of Q_i different from zero would point to NP in an unambiguous way, confirming the violation of lepton flavour universality observed in R_K. In addition B_5 and B_{6s} exhibit only a linear dependence on $C_{9\ell}$ at large recoil providing further possibilities to disentangle the contributions coming from NP in

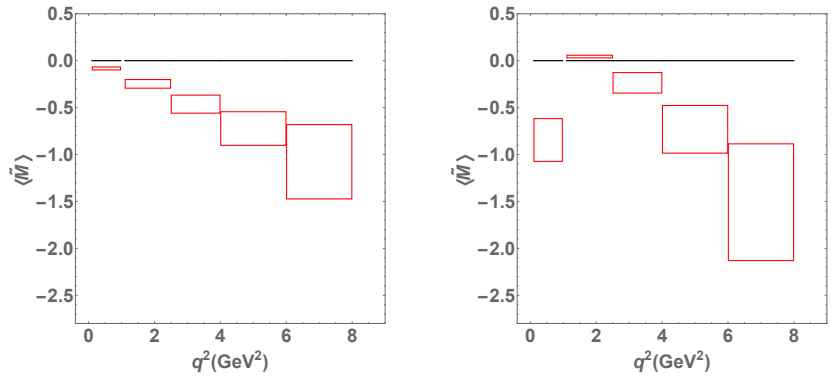

Figure 5: Predictions (in red) for the observable $\tilde{M}$ in two different NP scenarios violating lepton-flavour universality: $\mathscr{C}_{9\mu}^{\rm NP} = -1.1, \mathscr{C}_{ie}^{\rm NP} = 0$ (left), $\mathscr{C}_{9\mu}^{\rm NP} = \mathscr{C}_{10\mu}^{\rm NP} = -0.65, \mathscr{C}_{ie}^{\rm NP} = 0$ (right). From Ref. [26].

C_9 and C_{10}, with a clean separation between lepton-flavour dependent (NP) and lepton-flavour universal (NP or SM long-distance) contributions to C_9. We can also build the observable $\widetilde{M}$

$$\widetilde{M} = \frac{(\beta_e^2 J_5^\mu - \beta_\mu^2 J_5^e)(\beta_e^2 J_{6s}^\mu - \beta_\mu^2 J_{6s}^e)}{\beta_e^2 \beta_\mu^2 (J_{6s}^\mu J_5^e - J_{6s}^e J_5^\mu)} \tag{3.1}$$

which exhibits very interesting features: in the presence of lepton-flavour non-universal NP in $C_{9\ell}$ or $C_{10\ell}$ only, the large-recoil expression for $\widetilde{M}$ is independent of long-distance lepton-flavour universal contributions (in particular transversity-independent charm contributions) and provides clean signals of NP. In Ref. [26], several NP scenarios compatible with the global fit in Ref. [18] are disentangled with the help of these clean observables measuring lepton-flavour non-universality.

4. Conclusions

LHCb data on $b \to s\ell^+\ell^-$ decays shows several tensions with SM predictions, in particular in the angular observable P_5' of $B \to K^*\mu^+\mu^-$, in the branching ratio of $B_s \to \phi\mu^+\mu^-$, and in the ratio R_K (all of them at the $\sim 3\sigma$ level). In global fits of the Wilson coefficients to the data, scenarios with a large negative $\mathscr{C}_9^{\rm NP}$ are preferred over the SM by $\sim 4\sigma$ typically. A bin-by-bin analysis demonstrates that the fit is compatible with a q^2-independent effect generated by high-scale new physics, though a q^2-dependent QCD effect cannot be excluded with the current precision. Note, however, that a QCD effect could not explain the tension in R_K. The latter observable further favours a lepton-flavour non-universal scenario with NP coupling only to $\mu^+\mu^-$ but not to e^+e^-, a scenario to be probed by a measurement of analogous ratios for other observables.

Acknowledgments

This work received financial support from the grant FPA2014-61478-EXP [SDG, JM, JV]; from the grants FPA2013-46570-C2-1-P and 2014-SGR-104, and from the Spanish MINECO under the project MDM-2014-0369 of ICCUB (Unidad de Excelencia "María de Maeztu") [LH]; from DFG within research unit FOR 1873 (QFET) and from CNRS [JV]; from the EU Horizon 2020 programme from the grants No 690575, No 674896 and No. 692194 [SDG].

References

[1] R. Aaij *et al.* [LHCb Collaboration], JHEP **1602** (2016) 104.

[2] S. Descotes-Genon *et al.*, JHEP **1301** (2013) 048, JHEP **1305** (2013) 137.

[3] **LHCb** Collaboration, PRL **111** (2013) 191801.

[4] A. Abdesselam *et al.* [Belle Collaboration], arXiv:1604.04042 [hep-ex].

[5] **LHCb** Collaboration, Phys. Rev. Lett. **113** (2014) 151601.

[6] **LHCb** Collaboration, JHEP **1307** (2013) 084.

[7] F. Kruger and J. Matias, Phys. Rev. D **71** (2005) 094009.
B. Grinstein and D. Pirjol, Phys. Rev. D **70** (2004) 114005.

[8] J. Matias *et al.* JHEP **1204** (2012) 104.

[9] C. Bobeth, G. Hiller and D. van Dyk, JHEP **1007** (2010) 098.

[10] A. Bharucha, D. M. Straub and R. Zwicky,

[11] A. Khodjamirian *et al.*, JHEP **1009** (2010) 089.

[12] J. Lyon and R. Zwicky, arXiv:1406.0566 [hep-ph].

[13] M. Ciuchini *et al.*, JHEP **1606** (2016) 116.

[14] A. Ali, G. F. Giudice and T. Mannel, Z. Phys. C **67** (1995) 417.
G. Hiller and F. Kruger, Phys. Rev. D **69** (2004) 074020.
S. Descotes-Genon *et al.* , JHEP **1106** (2011) 099.
W. Altmannshofer, P. Paradisi and D. M. Straub, JHEP **1204** (2012) 008.
C. Bobeth, G. Hiller and D. van Dyk, Phys. Rev. D **87** (2013) 034016.

[15] S. Descotes-Genon, J. Matias and J. Virto, Phys. Rev. D **88** (2013) 074002.

[16] W. Altmannshofer and D. M. Straub, Eur. Phys. J. C **73** (2013) 2646.

[17] F. Beaujean, C. Bobeth and D. van Dyk, Eur. Phys. J. C **74** (2014) 2897 [Eur. Phys. J. C **74** (2014) 3179].

[18] S. Descotes-Genon *et al*, JHEP **1606** (2016) 092.

[19] R. R. Horgan *et al.*, Phys. Rev. D **89** (2014) 9, 094501; PoS LATTICE **2014** (2015) 372.
C. Bouchard *et al.*, Phys. Rev. D **88** (2013) 5, 054509 [Phys. Rev. D **88** (2013) 7, 079901].

[20] S. Descotes-Genon *et al.*, JHEP **1412** (2014) 125.

[21] S. Jäger and J. Martin Camalich, JHEP **1305** (2013) 043.

[22] W. Altmannshofer and D. M. Straub, Eur. Phys. J. C **75** (2015) 8, 382; arXiv:1503.06199 [hep-ph].

[23] T. Hurth, F. Mahmoudi and S. Neshatpour, Nucl. Phys. B **909** (2016) 737,

[24] R. Aaij *et al.* [LHCb Collaboration], JHEP **1504** (2015) 064.

[25] G. Hiller and M. Schmaltz, Phys. Rev. D **90** (2014) 054014; JHEP **1502** (2015) 055.
D. Ghosh, M. Nardecchia and S. A. Renner, JHEP **1412** (2014) 131.
T. Hurth, F. Mahmoudi and S. Neshatpour, JHEP **1412** (2014) 053.
S. Jäger and J. Martin Camalich, Phys. Rev. D **93** (2016) no.1, 014028.
D. Bečirević, S. Fajfer and N. Košnik, Phys. Rev. D **92** (2015) no.1, 014016.

[26] B. Capdevila *et al.*, arXiv:1605.03156 [hep-ph].